



# Journal of Applied Sciences

ISSN 1812-5654

**science**  
alert

**ANSI***net*  
an open access publisher  
<http://ansinet.com>

## Dynamic Modeling and Simulation of Ionic Polymer Metal Composites (IPMC) Actuated Manipulator

Khattak Muhammad Farid, Zhao Gang, Tran Linh Khuong and Zhuang-Zhi Sun  
College of Mechanical Engineering, Harbin Engineering University, 145-1 Nantong Street,  
Nangang, Harbin, 150001, Heilongjiang, People's Republic of China

**Abstract:** Ionic Polymer Metal Composites (IPMC) are soft and flexible materials that can produce large bending when low voltage is applied to them. This bending motion in parallel configuration enables the material to produce actuating force at the tip of the material strips. This characteristic of IPMC makes these materials suitable for multiple applications in industrial, medical, biological and biomimetic fields. In this study four different contributions are made. Firstly, a complete dynamic model has been developed to propose the ionic polymer metal composites as an actuating link for a two link bionic linkage of a manipulator as there was no such model before. The equations of motion are derived by using Lagrangian mechanics for the ionic polymer metal composite actuated two links manipulator joint. Secondly, a pair of ionic polymer metal composite strips is proposed as the actuating link to cater for the low force generation. Thirdly, the finite difference method is utilized for the solution of the model. Finally, the performance of the model is examined with numerical simulations built on time and frequency based simulation results for three different cases. Since, the aim of the model is to design a physical linkage where the force for the physical joint is provided by IPMC, therefore, the effect of increasing the mass of the second link has been analyzed with the same material properties comprising the initial link. Our results indicate that the mass of the second link is inversely proportional to the angle moved by it, whereas the kinetic and potential energies are directly proportional. Link-2 lags in time interval as compared to link-1, since link-1 is the driving link. The frequency-based analysis exposed that increasing mass of the link causes an increase in the vibrating frequency. These results anticipate that ionic polymer metal composite has sufficient potential to provide the force for the movements of manipulator links and can be employed to micro-scaled, multiple-joint manipulators to open a gateway for practical purposes.

**Key words:** Dynamic modeling, ionic polymer metal composite, bionic joint, flexible linkage, electro active polymer, finite difference method, wolfram mathematica

### INTRODUCTION

The processes, physical systems and devices and the resultant models that are inspired and developed after the analysis of nature are named as "biomimetic". Due to the research and development in the field of automation, lightweight and energy-efficient robotic structures have been increasingly comprehended for tasks in medical, industrial and special-purpose military performances (Shahinpoor and Kim, 2005; Kim *et al.*, 2009).

Flexible actuators are good contenders for microminiaturized devices. Ionic Polymer Metal composite (IPMC) is an Electroactive Polymer (EAP) and has attracted several researchers for application in many medical and industrial fields (Nemat-Nasser and Li, 2000; Bonomo *et al.*, 2006). IPMCs are light-weighted, flexible, swiftly actuated, active at low voltage, efficient in

underwater applications and dynamics in any direction (Takenaka *et al.*, 1982; Punning *et al.*, 2009). They possess high toughness with enormous actuation strain and intrinsic vibration hampering. These properties of IPMC make them suitable for utilization in microminiaturized devices.

The major portion of an IPMC consists of a polymer membrane which is coated with thin metallic layers on both sides. Under a suddenly applied step function (1 to 3 Volt), the IPMC displays a fast bending motion towards the anode followed by a slow relaxation (Wu and Nemat-Nasser, 2004). Similarly, a reversal in the voltage direction reverses the actuator bending. Due to the above-mentioned advantages of IPMC; the application scope of IPMC is increasing progressively. IPMC's prospective application range includes; surface and underwater robotic sensors, mechanical, biomedical,

mechano-electrical and energy reaping transducers (Abedi *et al.*, 2008; Asaka *et al.*, 1995).

Currently, the research in IPMCs is being carried out in two different directions. In the first case, the researchers deal with the performance-enhancement techniques in order to remove the deficiencies, improve the force generation of the actuators and increasing the life cycle of the IPMC strips (Asaka and Oguro, 2000). Similarly, in the second direction, the research is concerned with the application areas of the IPMC material actuator and sensors (Nemat-Nasser, 2002; Shahinpoor and Kim, 2002).

However, in the application fields, very little work has been carried out on presenting the mathematical models of the actuator, including the kinematics and dynamic models (Newbury and Leo, 2003; Weiland and Leo, 2005).

In this study, four different contributions are made:

- Firstly, IPMC is proposed as an actuating link for a small manipulator followed by the development of the dynamic model of the proposed application. IPMC has been considered as a link of the manipulator
- Secondly, a pair of IPMC strips is proposed as an actuating link to cater for the low force generation.
- Thirdly, the dynamic model has been developed through the “Lagrangian formulation” for the manipulator and has been solved through finite difference method
- Finally, simulation results are achieved and their analysis is carried out

### DYNAMIC MODELING

IPMC can be useful to provide the force for the movements of adjoining links of small manipulators to imitate the bionic joints of insects like grasshoppers etc. due to their small force requirement. Due to a parallel pairing setup of its actuators, IPMC can also be applied to provide the required force for their movements of the links. As depicted in Fig. 1, the two strips of IPMC are attached to a rigid bar. The flexible IPMC strips embody the first link of manipulator, whereas the rigid inclined bar represents the leg (second link) of the grasshopper manipulator. The force produced by the IPMC strips is used to provide the up and down motion to the rigid link through a pinion joint support at the middle.

The strips are fixed to the bar in parallel to achieve a linear motion. In this study, the dynamic model has been presented for the stretched position of the design by using Lagrangian method and Simulation results are presented for the validation of the model. Due to the symmetric structure of both IPMC strips, the dynamic effects of only one actuator are considered. The effect of

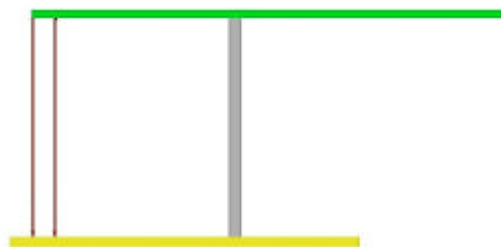


Fig. 1: Proposed model before bending

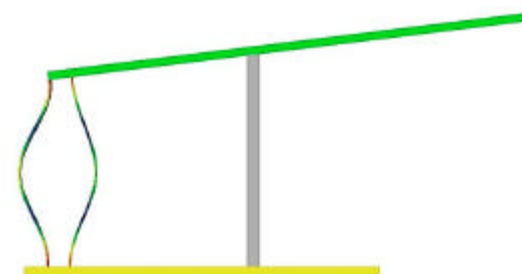


Fig. 2: Proposed model after bending

the pinion support for the model is also assumed to be negligible and hence ignored.

Considering this two link model presented in the Fig. 2, it can be seen that link 1 is flexible (IPMC) while the second link is rigid. It is indicated that after the application of voltage, the bending of the IPMC actuator link has resulted the upward movement of the second link through an angle of  $\theta_2$ . The dynamics of the model involves calculating as how the mechanism will move under the application of joint torques  $\tau_1$  and  $\tau_2$ . This includes the calculation of joint angles  $\theta_1$  and  $\theta_2$ , potential and kinetic energies  $P_1$ ,  $P_2$ ,  $K_1$  and  $K_2$  for link 1 and link 2, respectively. Where  $L_1$  and  $L_2$  are the corresponding lengths of the links. The position vector of link 1 is represented by  $r$ . The equations of kinetic and potential energies of both links are derived in the subsequent sections 1 to 4.

**Kinetic energy of link 1:** Since both the IPMC actuators are symmetrical, hence for simplicity, we have considered the model of one strip. Since the first link is flexible and so it is essential to find its translational and rotational velocities. For this, the translational kinetic energy is denoted by  $K.E_{1(\text{translational})}$  and its x and y components are represented in Cartesian coordinate system as shown in the Fig. 3 and are given in Eq. 1:

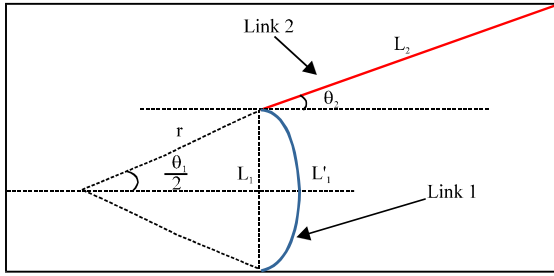


Fig. 3: Schematic diagram of the model

$$[x_1, x_2] = \left[ r \cos\left(\frac{\theta_1}{2}\right), r \sin\left(\frac{\theta_1}{2}\right) \right] \quad (1)$$

The velocity components of translational kinetic energy are shown in Eq. 2:

$$[\dot{x}_1, \dot{y}_1] = [V_x, V_y] = \left\{ \dot{r} \cos\frac{\theta_1}{2} - \frac{r}{2} \sin\frac{\theta_1}{2}, 2\dot{r} \sin\frac{\theta_1}{2} + r \cos\frac{\theta_1}{2} \right\} \quad (2)$$

where,  $r$  and  $\theta_1$  is the function of time  $t$ .

The translational kinetic energy of link 1 is obtained by substituting the values of velocity components from Eq. 2 in 3:

$$K.E_{1(\text{translational})} = \frac{1}{2} (m_1 v_1^2) \quad (3)$$

Due to the flexing effect of Link 1, it possesses the rotational kinetic energy due to the angle  $\theta_1$  subtended after the application of the force and given in Eq. 4:

$$K.E_{1(\text{translational})} = \frac{1}{2} (m_1 r^2 \dot{\theta}_1^2) \quad (4)$$

The total kinetic energy  $K_1$  of link 1 becomes:

$$K_1 = K.E_{1(\text{translational})} + K.E_{1(\text{translational})}$$

Hence, the total energy of link 1 is shown in Eq. 5:

$$K_1 = \frac{1}{2} m_1 \{v_1^2 + r^2 \dot{\theta}_1^2\} \quad (5)$$

**Potential energy for link 1:** In order to find the potential energy of link 1 Eq. 6, Fig. 4 is considered. On the

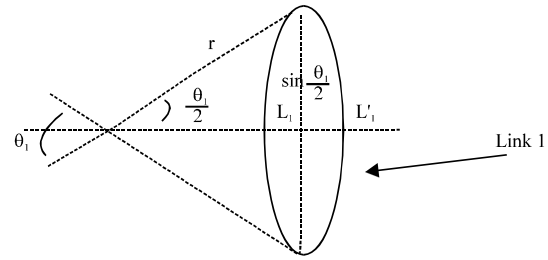


Fig. 4: Schematic diagram of Link 1

application of the specified voltage, it bends and makes an angle of  $\theta_1$  with a subtended radius  $r$ :

$$P_1 = m_1 g h = m_1 g (L_1 - L') \quad (6)$$

Where  $L_1 < L'$ , since the arc subtended by the radius  $r$  is  $S = L' = r\theta$ . Therefore, the potential energy of link 1 is given by Eq. 7:

$$P_1 = m_1 g \left( r\theta_1 - 2r \sin\frac{\theta_1}{2} \right) \quad (7)$$

**Kinetic energy for link 2:** The position vectors and velocities for link 2 in Cartesian coordinates are given in Eq. 8 and 9, respectively.

$$[x_2, y_2] = \left[ \left[ r \cos\frac{\theta_1}{2} + \cos\theta_2, \left( 2r \sin\left(\frac{\theta_1}{2}\right) + L_2 \sin\theta_2 \right) \right] \right] \quad (8)$$

$$[\dot{x}_2, \dot{y}_2] = [V_{2x}, V_{2y}] = \left[ \left\{ \left( \dot{r} \cos\frac{\theta_1}{2} \right) + \frac{1}{2} r \dot{\theta}_1 \sin\frac{\theta_1}{2} - L_2 \dot{\theta}_2 \sin\theta_2 \right\}, \left\{ \left( 2\dot{r} \sin\frac{\theta_1}{2} \right) + r\dot{\theta}_1 \cos\frac{\theta_1}{2} - L_2 \dot{\theta}_2 \sin\theta_2 \right\} \right] \quad (9)$$

Finally, the total kinetic energy of link 2 is described in Eq. 10:

$$K_2 = \frac{1}{2} m_2 \{m_2 v_2^2\} \quad (10)$$

**Potential energy for link 2:** To find the potential energy of link 2, author referred to Fig. 4. On the application of the specified voltage, Link 1 bends and subtends an angle with a subtended radius  $r$ . This changes the position of the link 2 and also its potential energy which is given in Eq. 11:

$$P_2 = m_2 g r \left( \theta_1 - 2r \sin \left( \frac{\theta_1}{2} \right) \right) + L_2 \sin \theta_2 \quad (11)$$

**Lagrangian formulation of the model:** Lagrangian formulation is a function that summarizes the dynamics of a system. To develop the dynamic model, the authors employed the Lagrangian formulation method explained in the present study. General form of Lagrangian is given in Eq. 12 below, where K is the kinetic energy and P represents the potential energy:

$$L_\alpha = \sum K - \sum P \quad (12)$$

Substituting the Eq. 5, 7, 10 and 11 in Eq. 12 above, gives the Lagrangian equation for the model.

The torques  $\tau_1$  and  $\tau_2$  as given in Eq. 13-14 are calculated by using the Lagrangian equation:

$$\tau_1 = \frac{d}{dt} \left\{ \left( \frac{\partial L_\alpha}{\partial \dot{\theta}_1} \right) - \left( \frac{\partial L_\alpha}{\partial \theta_1} \right) \right\} \quad (13)$$

$$\tau_2 = \frac{d}{dt} \left\{ \left( \frac{\partial L_\alpha}{\partial \dot{\theta}_2} \right) - \left( \frac{\partial L_\alpha}{\partial \theta_2} \right) \right\} \quad (14)$$

In matrix form, the final general dynamic equation for the model by using an IPMC strip link is shown in Eq. 15:

$$M(\theta)\ddot{\theta} + V(\theta)\dot{\theta} + C(\theta)\dot{\theta} = \tau \quad (15)$$

Where:

$$M(\theta)\ddot{\theta} = \begin{bmatrix} \frac{r^2}{8}(13+3\cos\theta_1)m_1 + (5+3\cos\theta_1)m_2 & \frac{r}{8} \left( 2\cos\left(\frac{\theta_1}{2}\right)\cos\theta_2 + \sin\left(\frac{\theta_1}{2}\right)\sin\theta_2 \right) L_2 m_2 \\ \frac{r}{2} \left( 2\cos\left(\frac{\theta_1}{2}\right)\cos\theta_2 + \sin\left(\frac{\theta_1}{2}\right)\sin\theta_2 \right) L_2 m_2 & L_2^2 m_2 \end{bmatrix} \quad (16)$$

$$V(\theta)\dot{\theta} = \begin{bmatrix} \frac{r}{4} \left( \frac{13+}{3\cos\theta_1} \right) m_1 \dot{\theta}_1 + \left( \frac{5+}{3\cos\theta_1} \right) m_2 \dot{r} - \frac{13}{16} r^2 \sin\theta_1 \left( \frac{m_1}{m_2} \right) \dot{\theta}_1^2 + \frac{r}{2} \left( \frac{\sin\left(\frac{\theta_1}{2}\right)\cos\theta_2}{2\cos\left(\frac{\theta_1}{2}\right)\sin\theta_2} \right) \dot{\theta}_1 L_2 m_2^2 \dot{\theta}_2 \end{bmatrix} \quad (17)$$

And:

$$C(\theta) = \begin{bmatrix} 3\sin\theta_1 m_2 \ddot{r} + m_1 + m_1 \left( 16g \sin\theta_1^2 + 3\sin\theta_1 \ddot{r} \right) \\ L_2 \left( \cos\theta_2 + \left( 2\cos\theta_2 \sin\left(\frac{\theta_1}{2}\right) - \cos\left(\frac{\theta_1}{2}\right)\sin\theta_2 \right) m_2 \ddot{r} \right) \end{bmatrix} \quad (18)$$

## SIMULATION RESULTS

In this section, three difference cases have been considered for the simulation of presented model on the base of time and frequency. The input torque is responsible for the dynamic behavior of the bionic joint (link-2). The torque is provided by the force generated by the IPMC strips (link-1). The IPMC actuator is very complex. It is non-linear with great hysteresis. First of all, the model is prepared for the system and obtained the expressions for kinetic and potential energy. The Lagrangian of the system are obtained from the two types of energies of each link. In this way, a highly non-linear coupled system of differential equations was achieved for which the exact solution would be nearly impossible. For this reason, a finite difference method was employed by changing the derivate into differential equations. This rendered the system into a non-linear algebraic system of equations. These equations are solved by using known initial and boundary conditions in a two step-approach. In the first step, equations are solved for the initial solution by using initial and known boundary conditions, while in the second step; the results are obtained for the next solution on the base of calculated results obtained in the first step. Similarly, the results for the  $n^{\text{th}}$  solution were obtained from  $n^{\text{th}-1}$  and  $n^{\text{th}-2}$  solutions iteratively.

In the solution, the input values of  $L_1$ ,  $L_2$ ,  $m_1$ ,  $\tau_1$  and  $\tau_2$  are constant, while the value of  $m_2$  is changing in each case. The analysis is made by the difference of the results for each run of the simulation model. The application of initial boundary conditions of  $\text{del}(\Delta) = 0.001$ ,  $\theta_1(0) = 0.5$  and  $\theta_2(0) = 0$  provided the simulation results as shown in Fig. 5-22 calculated in the three cases. The initial boundary conditions were also retained the same in all the three cases.

**Case 1:** For case 1, the initial values of  $m_1$ ,  $m_2$ ,  $\tau_1$  and  $\tau_2$  are selected as shown in Table 1. Since, the IPMC link is lighter than the leg of the grass-hopper; so it is selected six times lighter for this case. The simulation results performed are highlighted in the graphs shown in the Fig. 5-10.

Since link-1 has a lesser mass than that of link 2 and the same is reflected in the resultant graphs, where  $K_1$  is

Table 1: Simulation parameters

Parameters	$m_1$ (mg)	$m_2$ (mg)	$\tau_1$ (Nm)	$\tau_2$ (Nm)	$L_1$ (mm)	$L_2$ (mm)
Case 1	80	500	0.5	0.1	50	80
Case 2	80	525	1	0.1	50	80
Case 3	80	550	1	0.1	50	80

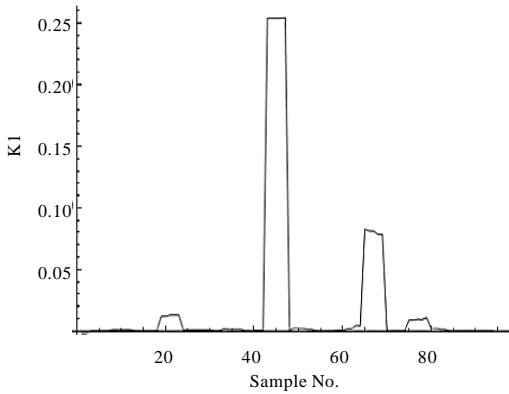


Fig. 5: Kinetic energy of link 1

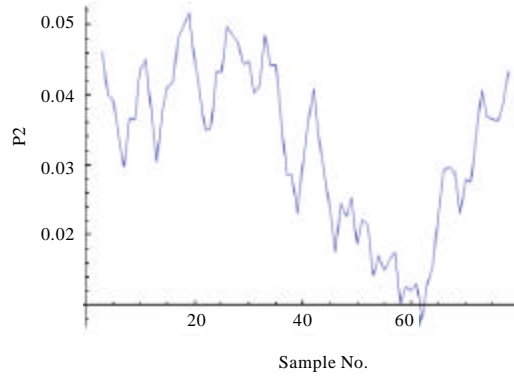


Fig. 8: Potential energy of link 2

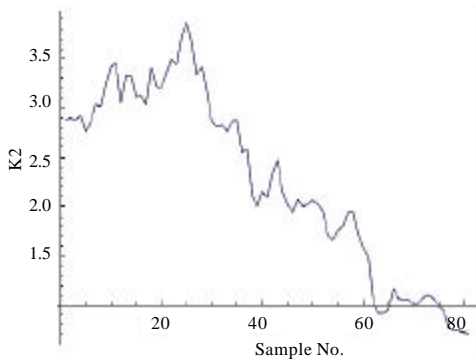


Fig. 6: Kinetic energy of link 2

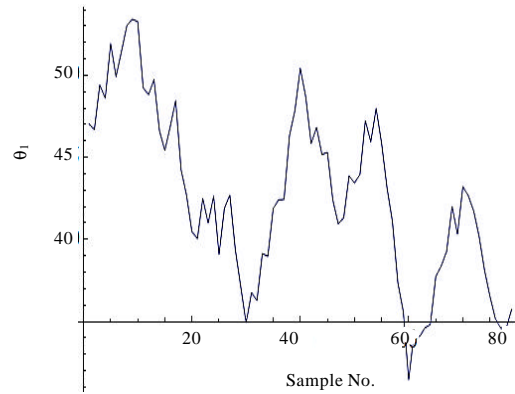


Fig. 9: Angle subtended by link 1

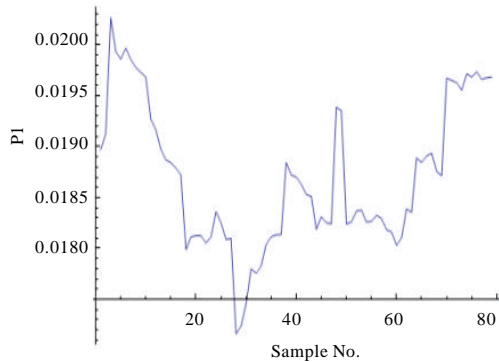


Fig. 7: Potential energy of link 1

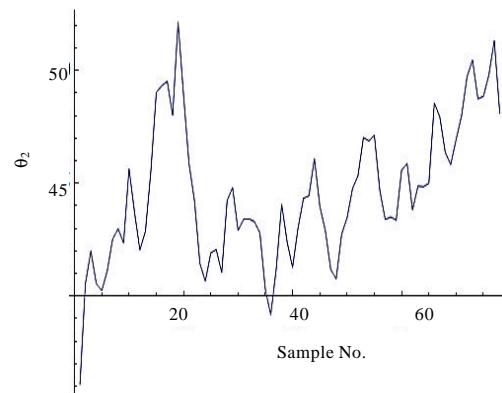


Fig. 10: Angle graph of the rigid link 2

several order of magnitude lesser than  $K_2$ . The angle range of  $\theta_1$  for link 1 is between  $30-55^\circ$ , whereas,  $\theta_2$  remains between  $35-55^\circ$ . The curve of link 1 is relatively smooth as compared to that of link 2. The graph for angle of  $\theta_2$  for the rigid link indicates that it experiences a vibratory motion.

The graphs of potential energies for the two links indicate that both links achieve their maximum potential energies nearly at the same time. The potential energy of link-2 is more in magnitude than that of link 1. It is

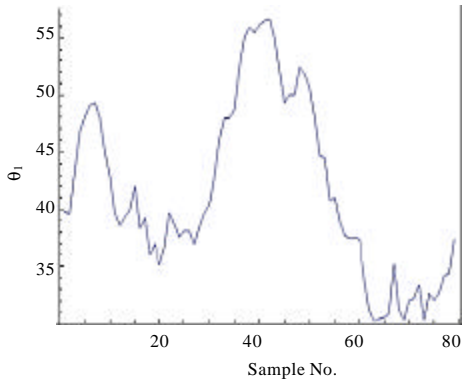


Fig. 11: Angle graph of link 1 (case 2)

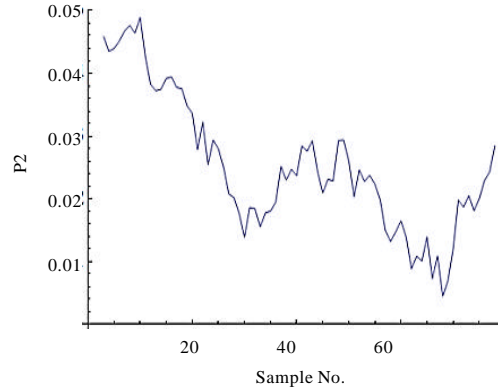


Fig. 14: Potential energy of link 2 (case 2)

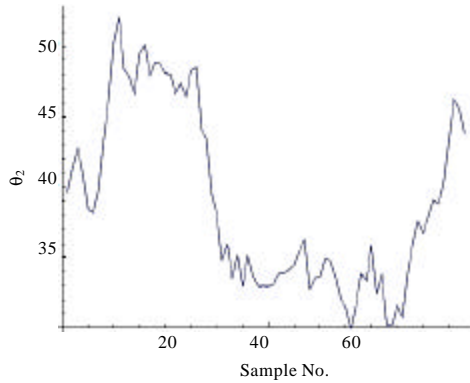


Fig. 12: Angle graph of link 2 (case 2)

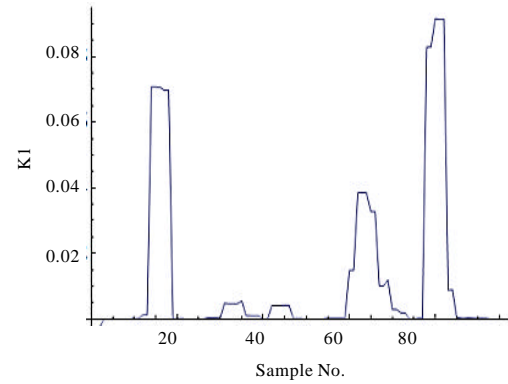


Fig. 15: Kinetic energy of link 1

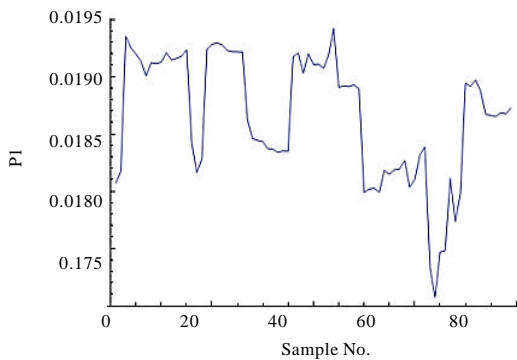


Fig. 13: Potential energy of link 1(case 2)

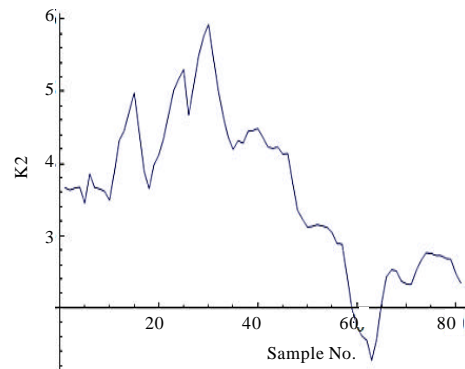


Fig. 16: Kinetic energy of link 2

attributed to the fact that it contains one more component than that of link-1 as shown in Fig. 4.

**Case 2:** In the case 2, the simulation parameters are changed in terms of the mass of link-2 as shown in Table 1. The mass of link-2 was increased from 500-525 mg, while keeping unchanged all other attributes. The simulation results are displayed from Fig. 11-16.

Here, the range of angles of  $\theta_1$  and  $\theta_2$  lies between  $35-55^\circ$  and  $30-55^\circ$ , respectively. The curve of link-2 is displaying a lag in time than that of link-1. It can be perceived that link-1 is demonstrating its maximum value at 40th sample; whereas at the same instant, the angle of link-2 is nearly at minimum at that point. Both the curves are approximately following the same time trend after approaching the 60th sample.

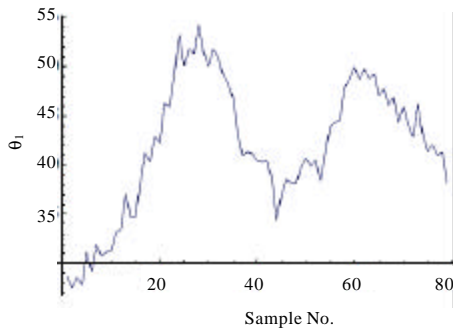


Fig. 17: Angle graph of link 1 (case 3)

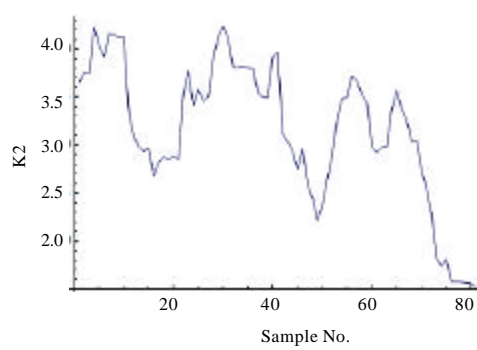


Fig. 20: Kinetic energy of link 2 (case 3)

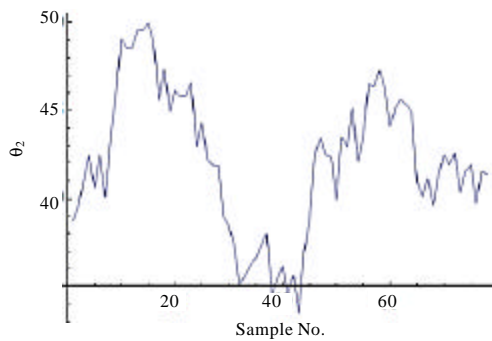


Fig. 18: Angle graph of link 2 (case 3)

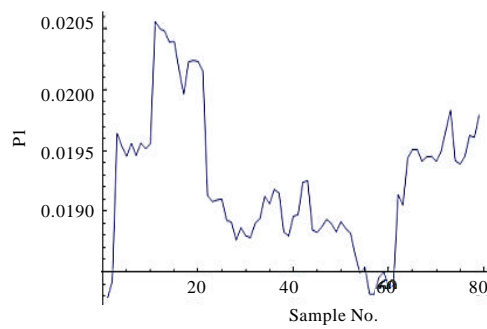


Fig. 21: Potential energy of link 1 (case 3)

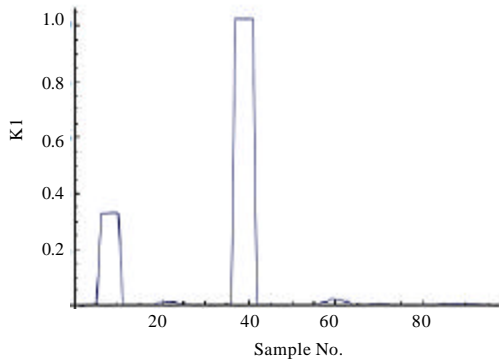


Fig. 19: Kinetic energy of link 1 (case 3)

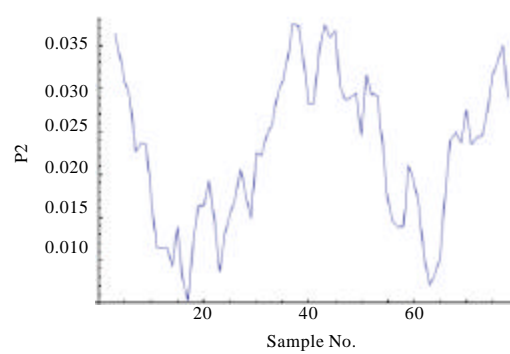


Fig. 22: Potential energy of link 2 (case 3)

In case of kinetic and potential energies, link-2 is demonstrating to have more energy as that was the situation in the earlier case. The curves for link-1 are showing some stability at some interval of time before reaching its minimum values, after which it can be seen to climbing up again. The potential energy of link-2 decreases smoothly to its minimum in contrast to link-1. The kinetic and potential energy of link -2 are also greater than that of link-1 as in case 1. Because of the low mass of IPMC, its kinetic energy is again unsubstantial similar to case-1. Link-1 is presenting an abrupt peak to display the sudden voltage application.

**Case 3:** As compared to case 2, the mass of link-2 is increased to 550 mg instead and retained the left over parameters. Now  $m_2$  and  $m_1$  are at approximate ratio of 7: 1 to each other. In the initial part of the simulation run, it can be observed that the angle subtended by link 2 is more than that of link 1. After that,  $\theta_2$  displays a decreasing trend with an increasing curvature of  $\theta_1$ , until they become approximately equal at 20th sample time interval. At 40th sample, the angles of both links reach their minimum value of  $35^\circ$ .

However, repeating crests and troughs can be observed in all the graphs to confirm the vibrating and



**Table 2: Modes frequencies**

Link 2 mass (g)	Mode frequencies(Hz)			
	Link-1		Link -2	
	Mode-1	Mode-2	Mode-1	Mode-2
500	21	11	43	7
525	9.9	12	45.1	13
550	41	27	44	41

non-linear nature of the model. The graphs of kinetic energies of the links are shown in Fig. 21-22. The energies of link-2 are much more than that of link-1. The energies of link 1 are found to be at minimum initially but those of link 2 are at the maximum and vice versa. This indicates that link 2 lags behind link 1 in time interval by some instant. A sudden peak in the velocity gradient of both the links can be found out. This phenomenon signifies the sudden bending of the IPMC strips upon the application of the voltage. All the graphs for link 2 are following the trend of link 1 with a slight delay in time to ensure that the moment of the first link energizes the following link.

To analyze the effects of gradually increasing the mass of link 2, it can be seen that initially the angle of link-2 decreases as the mass  $m_2$  approaches to 550 from 500 mg. For 500 mg, the link initial subtended angle is  $47^\circ$ ,  $40^\circ$  for 525 mg and below  $30^\circ$  for 550 mg. This verifies that heavier the link-2, the lesser is the subtended angle. The kinetic energy of the link increases with increasing the mass as it is the function of mass. It can be noted that the graphs are plotted at different masses. However, the potential energy decreases with increasing mass. This is mainly due to the reduced angle covered by the link with increasing mass.

Modes frequencies are also analyzed at these weights as shown in Table 2. Two mode frequencies are selected for each mass and the comparison is made. It can be seen that resonance modes of vibration of the system transfer to higher frequencies with increasing mass. This implies that the manipulator vibrates at higher frequency rates after increasing mass than those with low masses.

**CONCLUSION AND FUTURE WORK**

The described properties of the Ionic Polymer Metal Composite (IPMC) are a flexible, electroactive polymer material which displays a large bending motion on the application of low voltage. This characteristic of IPMC makes the material suitable for applications in different fields such as medical, industrial and special-purpose military performances etc. In this study, a fresh idea has been presented by the authors regarding the application of IPMC material to mimic the actuating knee joint muscles of the insects. For this, the IPMC itself has been considered first as a bionic manipulator link and pair of parallel strips of IPMC is also suggested to accommodate

for low force generation. And then the dynamic model has been developed through the “Lagrangian formulation” for the manipulator.

The proposed model has been solved by applying the finite difference method through two-step approach by using wolfram mathematica software. Finally, the simulation of the model has been carried out for three different scenarios (cases) and obtained different results of the model. Results of the simulation indicate that links dynamics are quite coherent. It showed that by increasing the mass of link 2, the angle range of the link decreases. It was also observed that the link 2 lag behind the link 1 in some time interval to validate that link 1 is energizing it and the kinetic and potential energies of link-2 increases with the increasing mass. The results obtained are very logical by considering the theoretical aspects. Since, the driving link (made of IPMC), provides the same force, hence by increasing the mass of the driven link must cover a lesser angle as compared to lesser mass of the driven link. Similarly, the driven mass should move after it has been supplied by a force by the driving link. The slight lag of the movement of the driven link validates this theory.

The mode frequency analysis indicates that the manipulator vibrates at higher frequency rates at increasing masses because of the flexible nature of the driving link. It can be concluded from the simulation results and mode frequency chart that Ionic Polymer Metal Composites can be utilized to provide the required force for actuating small manipulator’s links. As it was a set of highly non-linear coupled system of differential equations and the exact effect of one variable on the other was not known hence, the approximate values were used for the remaining variables. In our future study, we are planning to physically manufacture the proposed linkage and validate the model with experimental data. However, the proposed model has the potential for real life application and opens new avenues in the further research in these types of manipulator.

**ACKNOWLEDGEMENTS**

The study is support by the financial department of College of Mechanical Engineering, Harbin Engineering University and authors would like to express great thanks to Mr. Muhammad Hashim and Mr. Asim Ismail for their valuable suggestions and discussions.

**REFERENCES**

Abedi, E., A.A. Nadooshan and S. Salehi, 2008. Dynamic modeling of two flexible links manipulators. World Acad. Sci. Eng. Technol., 22: 461-467.

- Asaka, K. and K. Oguro, 2000. Bending of polyelectrolyte membrane platinum composites by electric stimuli: Part II. Response kinetics. *J. Electroanal. Chem.*, 480: 186-198.
- Asaka, K., K. Oguro, Y. Nishimura, M. Mizuhata and H. Takenaka, 1995. Bending of polyelectrolyte membrane-platinum composites by electric stimuli I. Response characteristics to various waveforms. *Polym. J.*, 27: 436-440.
- Bonomo, C., L. Fortuna, P. Giannone, S. Graziani and S. Strazzeri, 2006. Motion Sensors and Actuators based on Ionic Polymer-Metal Composites. In: *Device Applications of Nonlinear Dynamics*, Baglio, S. and A. Bulsara (Eds.). Springer, Netherlands, ISBN-13: 9783540338772, pp: 83-99.
- Kim, C.J., N.C. Park, H.S. Yang, Y.P. Park and K.H. Park Kim *et al.*, 2009. A model of the IPMC actuator using finite element method. *Electroact. Polym. Actuators Devices*, 7287: 1-7.
- Nemat-Nasser, S. and Y.J. Li, 2000. Electromechanical response of ionic polymer-metal composites. *J. Applied Phys.*, 87: 3321-3331.
- Nemat-Nasser, S., 2002. Micromechanics of actuation of ionic polymer-metal composites. *J. Applied Phys.*, 92: 899-915.
- Newbury, K.M. and J.D. Leo, 2003. Linear electromechanical model of ionic polymer transducers-Part I: Model development. *J. Intell. Mater. Syst. Struct.*, 14: 33-42.
- Punning, A., U. Johanson, M. Anton, A. Aabloo and M. Kruusmaa, 2009. A distributed model of Ionomeric polymer metal composite. *J. Intell. Mater. Syst. Struct.*, 20: 1711-1724.
- Shahinpoor, M. and K.J. Kim, 2002. Mass transfer induced hydraulic actuation in ionic polymer-metal composites. *J. Intell. Mater. Syst. Struct.*, 13: 369-376.
- Shahinpoor, M. and K.J. Kim, 2005. Ionic polymer-metal composites: IV. Industrial and medical applications. *Smart Mater. Struct.*, 14: 197-214.
- Takenaka, H., E. Torikai, Y. Kawami and N. Wakabayashi, 1982. Solid polymer electrolyte water electrolysis. *Int. J. Hydrogen Energy*, 7: 397-403.
- Weiland, L.M. and D.J. Leo, 2005. Computational analysis of ionic polymer cluster energetics. *J. Applied Phys.*, 97: 35-41.
- Wu, Y. and S. Nemat-Nasser, 2004. Verification of micromechanical models of actuation of Ionic Polymer-Metal Composites (IPMCs). *Smart Mater. Struct.*, 5385: 155-158.